# Experimental and FDM Study on Geogrid-Soil Interaction by Reformed Direct Shear Test Apparatus

**A. Namaei**[1*], **M. A. Arjomand**[1] **and A. Aminaee**[1]

1. Faculty of Civil Engineering, Shahid Rajaee Teacher Training University, Tehran, Iran

Corresponding author: *namaeiali@yahoo.com*

| ARTICLE INFO | ABSTRACT |
|---|---|
| | This paper presents the effect of geogrid tensile strength by computing the pullout resistance and the geogrid-soil interaction mechanism. In order to inquire this interface, a series of pullout tests have been conducted by a large scale reformed direct shear test apparatus in the both cohesive and granular soils. In numerical, the finite difference software FLAC3D has been carried out on experimental tests and the results are compared with findings from laboratory tests and to complete investigation results. The results reveal that the tensile strength of geogrids has a major role in the interface behavior. The effect of the soil type also is discussed. The acquired results indicate that the geogrids with low tensile strength have higher pullout resistance in the low normal stress on the surface, this effect reversed as the normal applied stress is increased. Numerical analysis only estimates the pullout strength with good agreement in the high normal stresses. Furthermore, it is found that the effective particle size of soil is close to the geogrid thickness by comparing two sands with different grain size. |

## 1. Introduction

Nowadays, geogrid materials have been employed in numerous reinforcement applications such as highways, railways and mine fields. These materials tend to increase the soil modulus by allocating the high shear resistance for the soil and geogrid composite. As the geogrids attach to a supporting structure like shotcrete, the induced loads mainly pass through the tensile resistance. Thus, one of the most common failure mechanisms is the pullout failure.

The pullout resistance behavior of geogrid includes: (1) the shear resistance inside of geogrid aperture; (2) the friction resistance between soil and longitudinal and transverse elements. A schematic view of resistance mechanism in geogrid is illustrated in Fig. 1, where LRs is the friction resistance between

soil and longitudinal elements, TRs indicates the friction resistance between soil and transverse elements and TRb presents the shear resistance inside of geogrid aperture. Pursuant to Bergado et al. [1], the total pullout resistance depends on the soil friction, the quasi geogrid friction, the geogrid shear to total shear ratio, the normal stress, and the total shear area. While the normal stress, the area of geogrid, and soil friction is constant. Therefore, the quasi geogrid friction should be computed accurately.
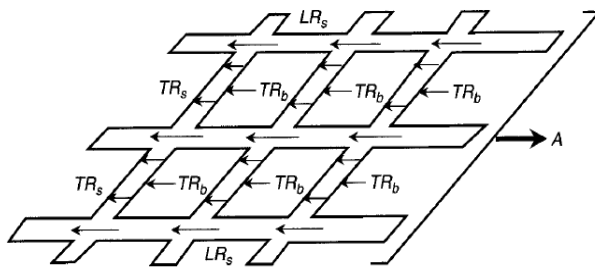


**Fig. 1.** Schematic view of resistance mechanism of geogrids [2].

The interfacial parameters have been inspected in different conditions by several researchers. [3 and 4]. The effect of the soil density and the normal stress was scrutinized by Lopez and Ladeira [5]. In their work, the geogrid-soil interface behavior has a significant effect on the geogrid mechanism. Abdi and Arjomand reinforced clay applying the geogrid embedded in a thin layer of sand. They found that a thin layer of sand covering the geogrids dramatically ameliorated the clay soil behavior through interfacial enhancement [6]. Naeini et al. assessed the interfacial parameters of geogrid in silty sand [7]. Liu et al. inspected these interfacial parameters in large scale [8].

In order to evaluate the geogrid-soil interface parameters, the pullout test has been employed by researchers [9-12]. Esfandiari and Selamat inquired on the transverse element of the geogrid and the differences with strip geogrids. According to their investigation, the passive shear resistance inside the geogrid apertures has a significant effect on the geogrid tensile behavior [13]. Bathurst and Ezzien also developed a new apparatus to assess the geogrid-soil interaction parameters [14]. Numerical analysis also has been applied in accordance with the experimental investigations by several researchers to develop a better consideration for the geogrid-soil behaviors [15 and 16]. Qian et al. explored numerically in conformity with their tests to assess the geogrid dynamical characteristic in ballast [17]. Wang et al. applied the DSM method for simulating geogrid-soil interaction, in the DSM method, the geogrid soil interaction has been observed by the force transfer accompanying the geogrid with different numbers of elements and soil [18].

All of the past studies were based on behavior of interaction parameters and pullout resistance in different conditions. However, none of the above researches have deliberated the effect of geogrid tensile strength on the pullout resistance. Thus, the effect of geogrid tensile strength on the pullout resistance is still is still in controversial.

The aim of this paper is to present the numerical and experimental results of pullout test on different geogrids strength in the coarse grain and fine grain soils with direct shear test apparatus by representing: (1) effect of geogrid tensile strength on geogrid-soil interaction; (2) effect of particle size of

sands on this interaction; (3) effect of type of soil.

## 2. Laboratory pullout tests and analyses

### 2.1 Soil

Two types of coarse grain and fine grain soil were applied in this research for contemplating possible aspects of interaction.

Kaolinite was used as the clay soil and Firzokooh sand was selected as the coarse grain soil. Two types of sand with different particle distribution were adopted in order to manifest the effect of particle size. The index properties of the clay and sand were computed in consonance with the appropriate ASTM standards and summarized in Table 1.

**Table 1.** Precise properties of soil used in this paper.

|       | D10 (mm) | D30 (mm) | D60 (mm) | ω (%) | γ (g/cm3) | φ (°) | c (kPa) |
|-------|------|------|------|------|------|------|------|
| Sand1 | 0.67 | 0.85 | 1.26 | 4.75 | 1.68 | 33 | 13.2 |
| Sand2 | 0.9 | 2.1 | 3 | 4.6 | 1.71 | 35 | 11.1 |

|      | LL (%) | PL (%) | PI (%) | | | | |
|------|--------|--------|--------|----|------|----|------|
| clay |        |        |        | 23 | 1.55 | 10 | 23.2 |
|      | 53 | 33.3 | 19.7 | | | | |

The procedures for specimen preparation and testing were standardized in order to achieve repeatability in the test results. All the initial tests were repeated until consistent results were obtained. The particle distribution results of these tests are demonstrated in Fig. 2.
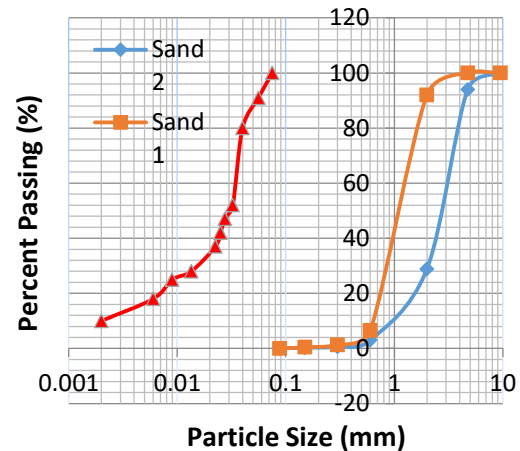


**Fig. 2.** Particles size distribution.

### 2.2 Test apparatus

The reformed direct shear test apparatus was invoked for inspecting the geogrid - soil interaction. In front of the bottom box has a groove with 6 mm height to pull out the geogrid. The PVC plate was appliedto prevent penetration of soil into the groove. In Fig. 3 a schematic view of the apparatus is depicted. The connection between the geogrid and the outer box was allocated with 6 bolts and a clamp. The bolts apply the pullout force on the geogrid. On the other hand, these bolts also provide fixity of geogrid (Fig. 4). The top part and the bottom part of a shear test box were connected to each other and were fixed at their position. Four buck shots and a steel plate were placed under the shear box to decrease the friction between the shear box and outer box (Fig. 5a).
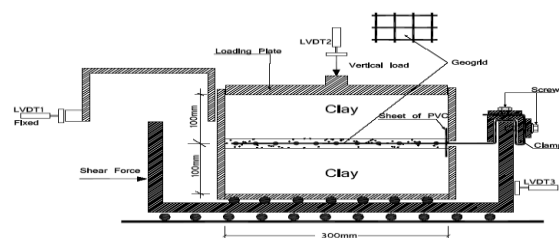


**Fig. 3.** Schematic views of reformed shear test apparatus.

**Fig**. **4.** Connection of geogrid with outer box.



(a) Steel plate under the shear box.



(b) Compacting layer of soil in shear box.

**Fig. 5.** Peppering experimental mode.

## 2.3 Test setup and programs

Samples were prepared by static compaction of soil to a predetermined dry density and moisture content (Fig. 5b). Accurately measured quantities of dry powdered soil and water corresponding to maximum dry density (MDD) and optimum moisture content (OMC) were thoroughly mixed and kept in plastic containers for 24 hours for uniform moisture distribution. Initially the lower half of the shear box was filled with three equal layers of soil and lightly tamped with the specially adopted tamping device. Subsequently geogrid specimen with the length to width ratio 2 covering the whole surface of the sample was horizontally laid and clamped to the inner face of the shear box. It is noteworthy to mention that the geogrid was apart 5 cm from the shear box body and the aperture sizes were assumed to be constant as a result to its effective role. The properties of four types of geogrid applied in this study are presented in Table 2. Each geogrid properties were acquired from its product sheet provided by the producer. Subsequently, the upper half of the shear box was positioned, secured and filled with moist soil in the same manner. After imposing the desired normal pressure and setting up gauges for measuring vertical and horizontal displacements as well as the shear force, testing commenced.

The engine generates a horizontal displacement with 1 mm/min velocity and for each 0.5 mm horizontal displacement, the force and the displacement gauges would be read for computing the tension force. The test would be continued up to the bolts horizontal displacement 2 cm. This displacement is for the beginning of the geogrid (near to the bits) and the pullout force was calculated from the ASTM D6706-01 recommendation presented in Eq. (1) where $P_r$ is the pullout resistance; $F_p$ is the pullout force; and $W_g$ is the geogrid width [19].

$$P_r = \frac{F_p}{W_g} \tag{1}$$

For measuring the geogrid tension displacement, the geogrid nodes were marked at the local coordinate system. At the final displacement, these marked nodes at the local coordinate system illustrated geogrid displacement.

**Table 2**. Properties of geogrid.

| Geogrid type | TG20-20 | TG55-30 | Fortrac | Miragrid |
|---|---|---|---|---|
| Tensile strength (KN/m) | 20 | 55 | 80 | 50 |
| Strain at nominal tensile strength in longitudinal direction | 13 | 13 | 12.5 | 11 |
| Thick (mm) | 1 | 1 | 2 | 2 |

In pullout tests three normal stresses were applied on four types of geogrids. The test programs conducted are given in Table 3. The constant horizontal displacement rate, the test time and the final displacement are recommended by ASTM D5321 [20]. The length and the width of the geogrids are different, because each types of the geogrid rolls applied in this study have a specific dimensions manufactured by their producer.

**Table 3.** Test program.

| Geogrid type | TG20-20 | TG55-30 | Fortrac | Miragrid |
|---|---|---|---|---|
| Length (cm) | 25 | 25 | 26 | 28 |
| Width (cm) | 12.5 | 12.5 | 13 | 14 |
| Normal stress (kPa) | 20,50,80 | 20,50,80 | 20,50,80 | 20,50,80 |
| Strain rate (mm/min) | 1 | 1 | 1 | 1 |
| Final displacement (mm) | 20 | 20 | 20 | 20 |
| Test time (min) | 20 | 20 | 20 | 20 |

## 3. Finite difference analysis

The finite difference program FLAC (Fast Lagrangian Analysis of Continua) 3D program was employed in order to assess the laboratory model results. FLAC enables users handling a wide range of Geotechnical problems. Due to non friction mobilization between the shear box and the outer box, only the shear box was modeled. The mesh size was selected by iteration until the mesh size did not affect the numerical results. The mesh sizes were adopted in accordance with the geogrid length and height 0.3 and 0.45 m, respectively. The mesh size was 0.35 m for the top part of the box and 0.33 m for the bottom part in conformity with the width direction. As the mesh size of the bottom and the top part has to be different in FLAC, the bottom part meshes were chosen finer. In this study, the Mohr-Coulomb criterion was employed for soil behavior and properties of soils were assigned in consonance with Table 1. The linearly elastic plate elements or geogrid structural elements was applied to model the geogrids reinforcement. It is noted that it would be more reasonable to assume the values of the friction and adhesion of the

geogrid-soil interface are deliberated as 2/3 φ and2/3c at the top and bottom of the geogrid. In addition, the normal and the shear stiffness are computed applying the FLAC recommendations as Eq. (2) where K and G are the bulk and shear modulus, respectively and zmin is the smallest width of an adjoining zone in the normal direction. In this study the normal and the shear stiffness were calculated as 8×105 kPa.

$$k_n = k_s = 10 \times \max[\frac{K+\frac{4}{3}G}{z_{min}}] \qquad (2)$$

All the boundaries were fixed in accordance with the three directions except from the groove portion of the shear box was free in all directions. A low velocity was applied on the geogrid in front of the groove to simulate the pull out force. The magnitude of this velocity was set to 2.5e-5 m/s in which the expected final displacement occurred. In Fig. 6 meshing of shear box and bold deformed mesh are illustrated which Fig. 6(b) displays the exaggerated geogrid pullout failure.
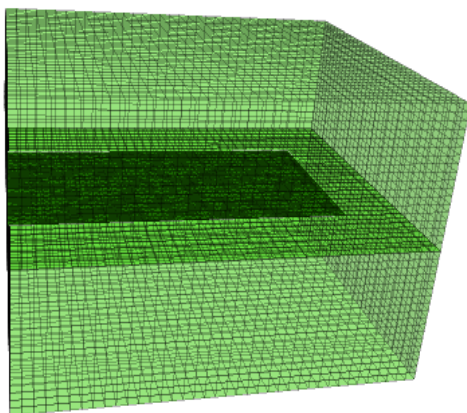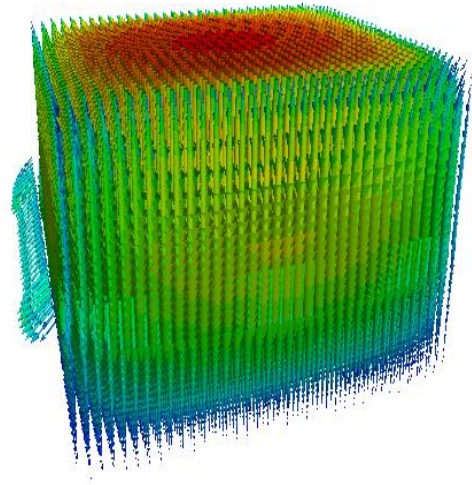


(b) Deformed mesh.

**Fig. 6.** Numerical model.

## 4. Results and discussion

For the geogrid-soil interaction investigation, 36 laboratory tests were conducted. An additional numerical study was analyzed on the geogrid in order to compare experimental results with numerical results. This illustrates the possibility of the pullout behavior prediction. It should be added that in this study, the maximum pullout force was deliberated as the pullout resistance.

### 4.1 Pullout resistance in sand

Fig. 7 displays the pullout force-displacement for sand1. It is clear that up to 1 mm displacement, there isn't noticeable difference between the pullout resistances of the geogrids. Then the pullout forces reach the maximum value slightly indicating the full pullout strength mobilization. Moreover, Fig. 7 indicates that the TG20-20 with 20 kN/m tensile strength in 20 kPa has higher pullout strength than 50, 55, and 80 kN/m geogrid resistances. It indicates that the TG20-20 has mobilized the ultimate



(a) Shear box meshing.

reinforcement resistance and the geogrid-soil interaction. In the other normal stresses, the strength mobilization increases as the geogrids strength increase. This phenomenon may be for the reason that the soil grains in the geogrid apertures are still in elastic phase under the 20kPa normal stress. Thus, the soil grains in the apertures interaction with the geogrid resistance (TRb) completely mobilize. Notwithstanding, the soil grains reach the plastic phase by losing their sharp corners when the normal stress increases. Therefore, the soil grains and aperture interaction decreases as the grains become rounded and under the 50, and 80 kPa, the higher tensile resistance play a significant role against pullout load.
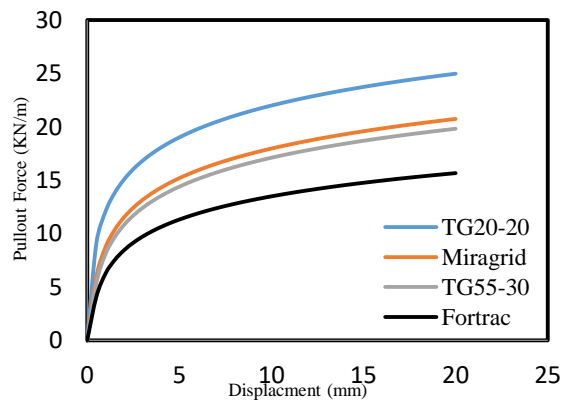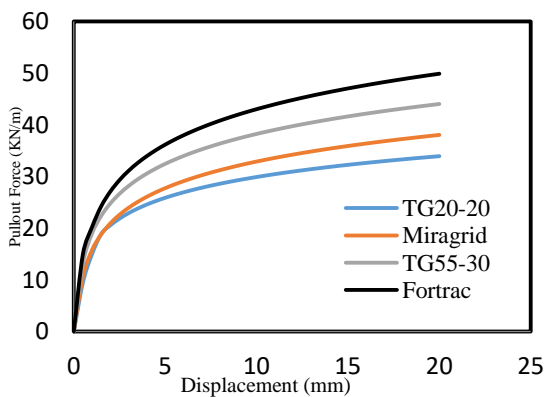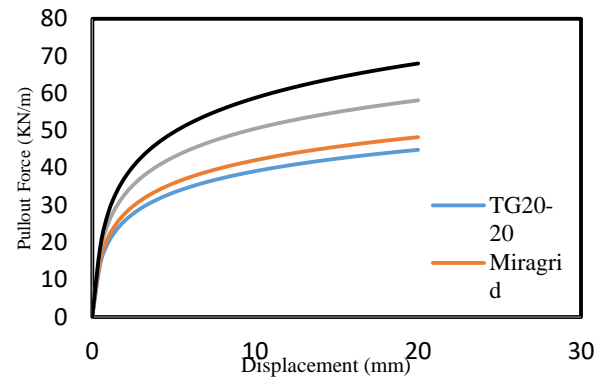
(c) 80 kPa.

**Fig. 7.** Laboratory pullout-displacement results on geogrids with different normal stress applied in sand1.

Fig. 8 illustrates the numerical results of the geogrid pullout-displacement. An evaluation on this graphs indicates that there is a good agreement between the numerical and the experimental results in 50, and 80 normal stresses (In the range of 1.1 to 1.2 higher than laboratory results). However, the pullout manner doesn't alternate in 20 kPa stress and the geogrid with higher tensile strength has the higher pullout resistance.

(a) 20 kPa.

(b) 50 kPa.

(a) 20 kPa.

(b) 50 kPa
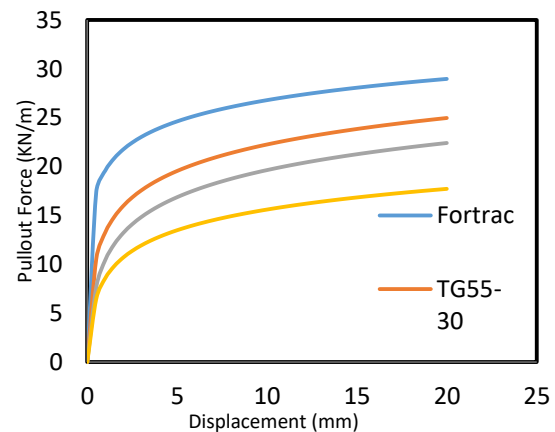

(c) 80 kPa.
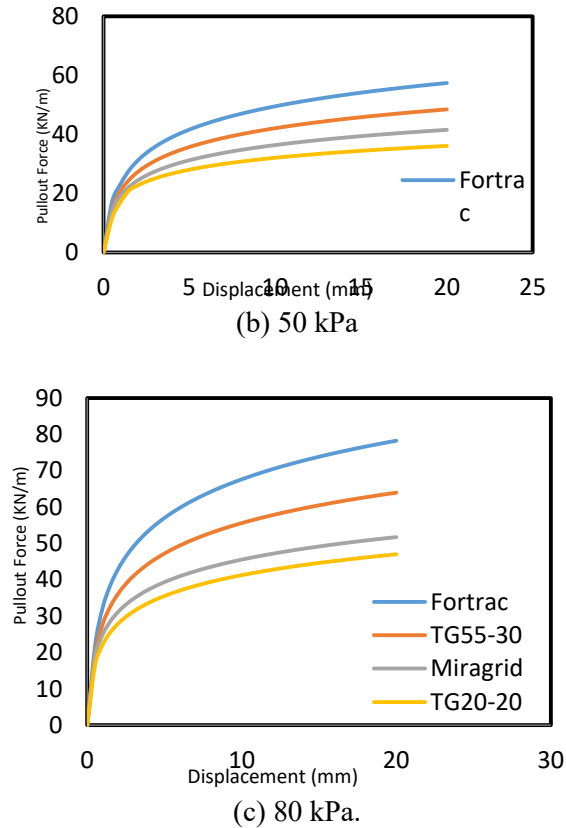
**Fig. 8.** Numerical pullout-displacement results on geogrids with different normal stress applied in sand1

In Fig. 9a the failure pushes are illustrated. There is a linear relationship between the normal stress and the pullout resistance. At the particular normal stress, the interaction behavior alternates and the geogrids with the higher tensile strength reveals the higher pullout strength. This graph shows that in the higher normal stresses, the particles of soil are compacted. Therefore, TRb increases and subsequently the geogrid pullout resistance increases. Pursuant to the failure pushes, the geogrids have some quasi cohesion. This cohesion is for the soil particle contact in the apertures of the geogrid creating as a result of suction in the soil. Quasi friction angle changes from 18 degree to 41 degrees in the geogrids.


(a) Sand1.
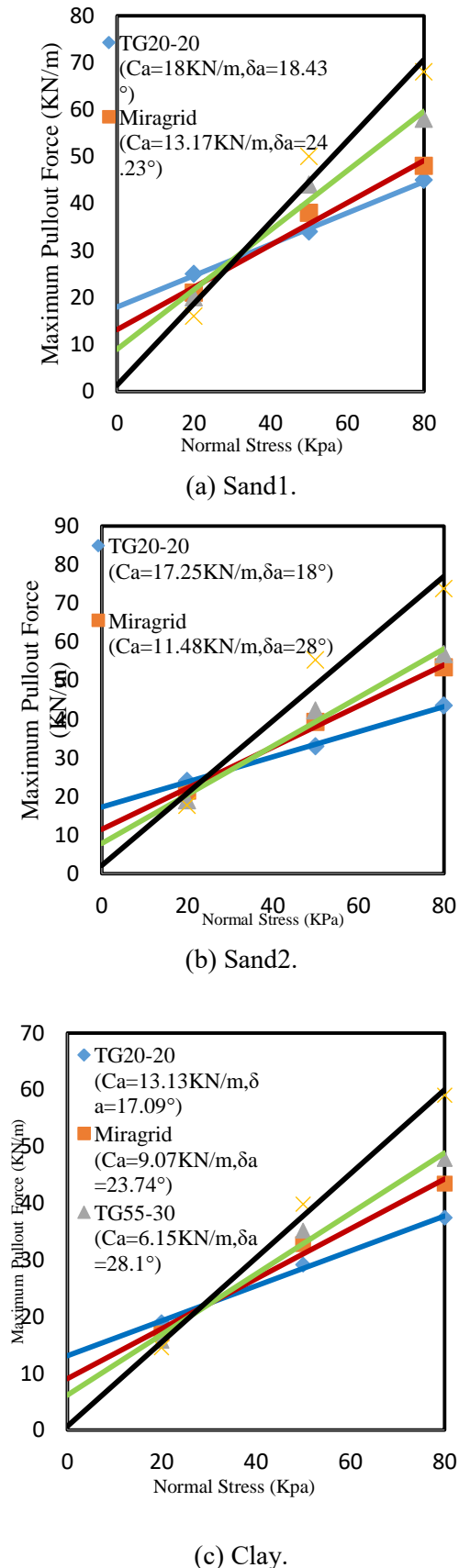

(b) Sand2.


(c) Clay.
**Fig. 9.** Laboratory failure pushes.

These mechanisms are same in sand2 (Fig. 10). After 1 mm displacement, the pullout force reaches the maximum value slightly which displays that the ultimate strength is mobilized completely and the grains in the apertures have the maximum interaction with the geogrid. Further, in 20 kPa normal stress, the pullout resistance of the geogrids with the lower strength increases. Fig. 9b indicates the failure pushes in sand2. The linear relationship is also like sand1. In addition, the quasi friction angle varies from 18 to 43 degrees.
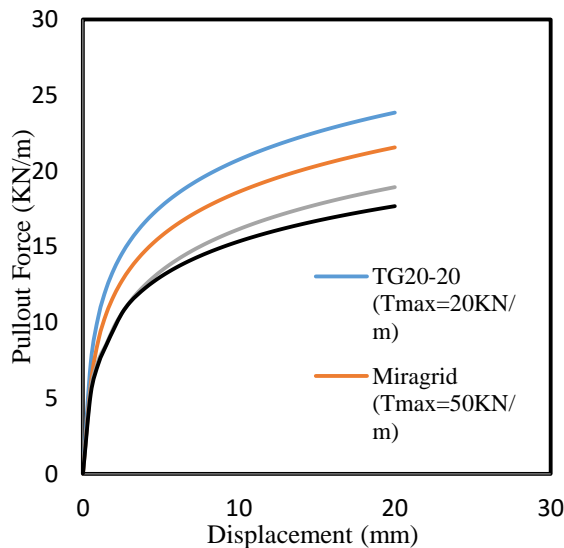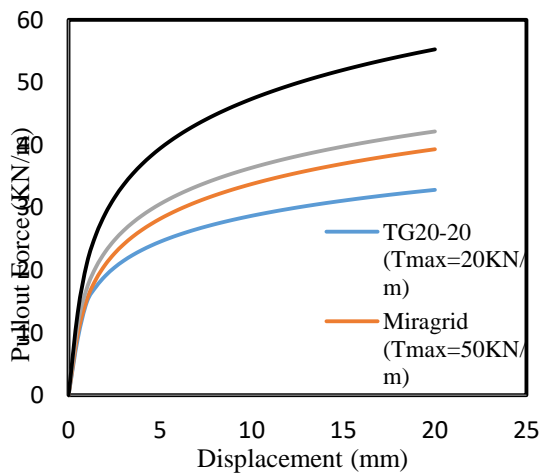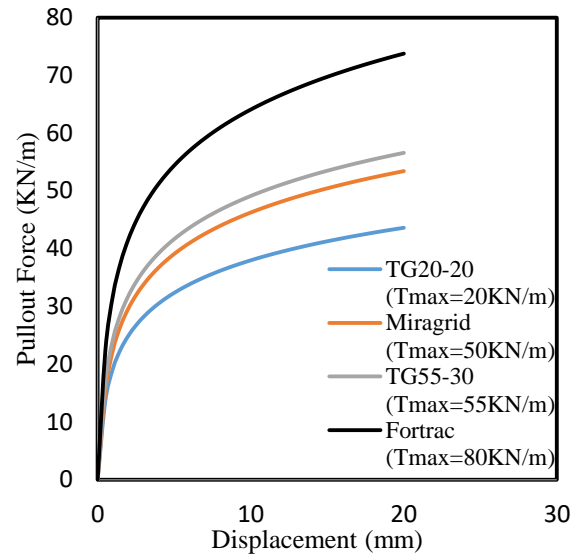

(c) 80 kPa.

**Fig. 10.** Laboratory pullout-displacement results on geogrids with different normal stress applied in sand2.

In Fig. 11 illustrates the numerical results of the pullout resistance in sand2. The numerical analysis doesn't separate behavior of 20 kPa stress with other stresses. The pullout resistances acquired from the numerical analysis were compared with the maximum laboratory resistance. in order to check this comparison, R parameter is described as Eq. (3).

$$R = \frac{\text{The maximum laboratory resistance}}{\text{The maximum numerical resistance}} \quad (3)$$

Here in Fig. 12, the large difference from one in value R manifests that the numerical analysis is inappropriate when it comes to estimating the pullout resistance and designing the geogrid reinforcement systems. Since the numerical analysis in 20 kPa normal stress does not deliberate the geogrid tensile strength effect in low normal stresses in the normal stress of 20 kPa, there is a huge disagreement for Fortrac and TG20-20 geogrids between laboratory and numerical results.
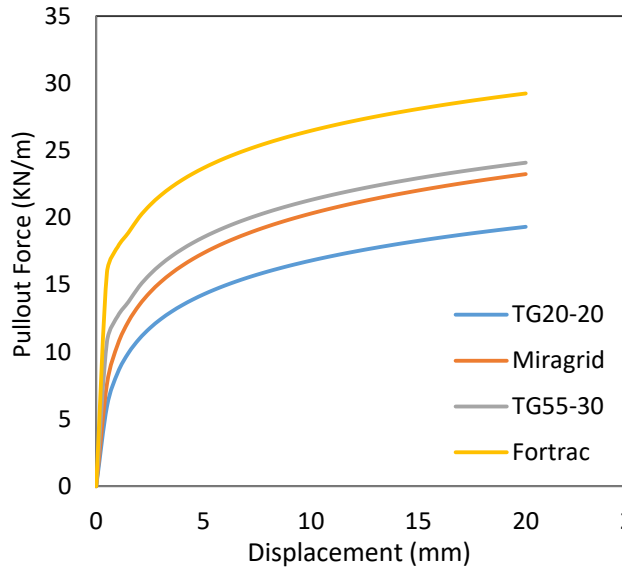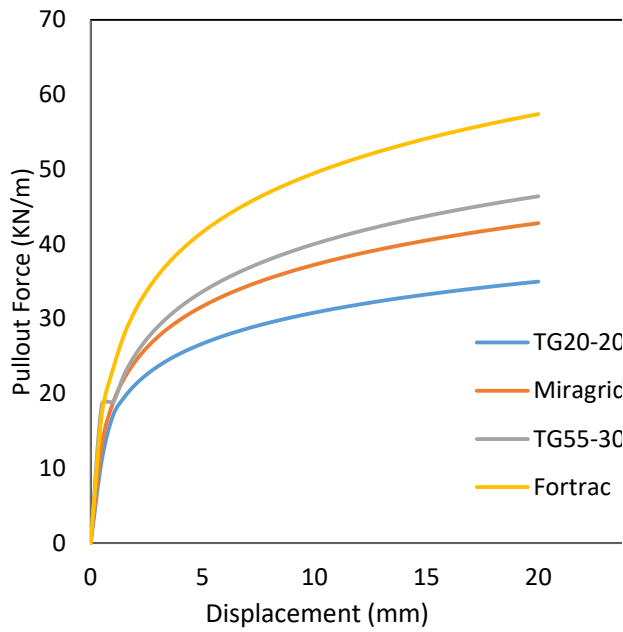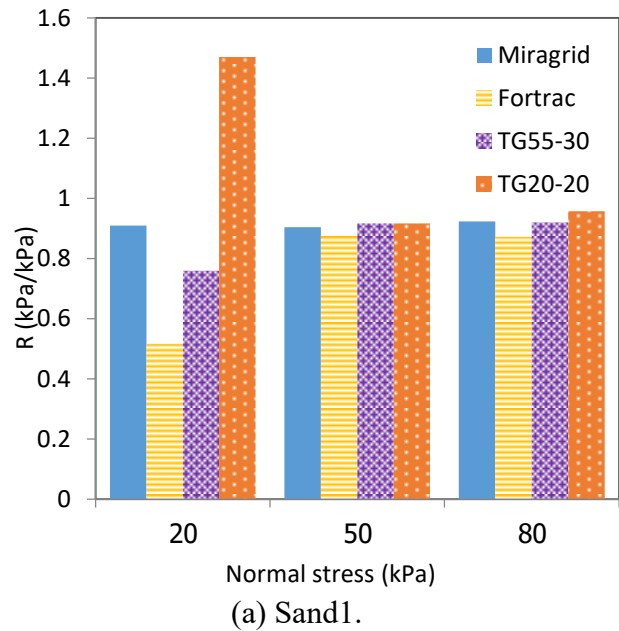

(a) 20 kPa.


(b) 50 kPa.

(a) 20 kPa.
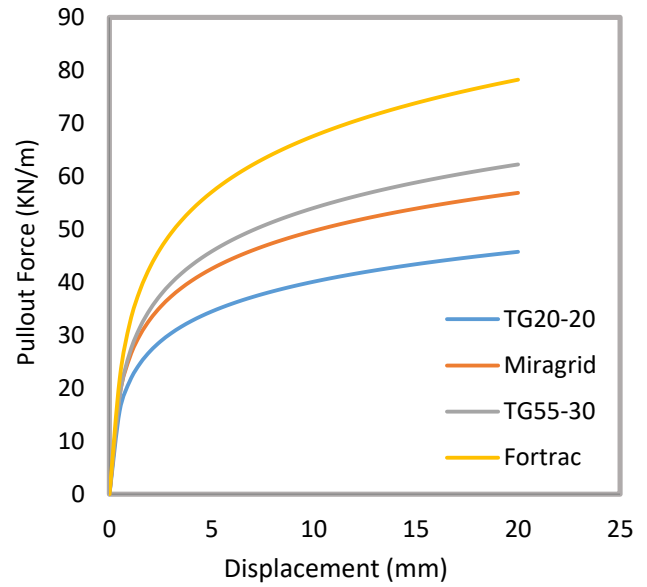


(c) 80 kPa.

**Fig. 11.** Numerical pullout-displacement results on geogrids with different normal stress applied in sand2.



(b) 50 kPa.
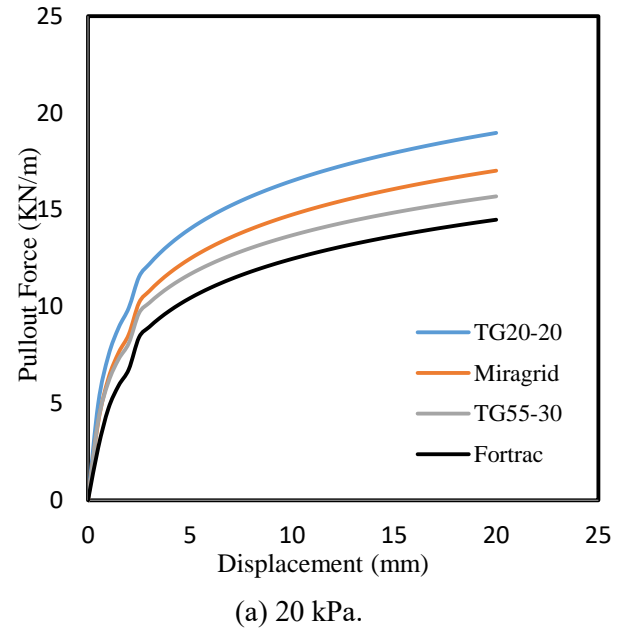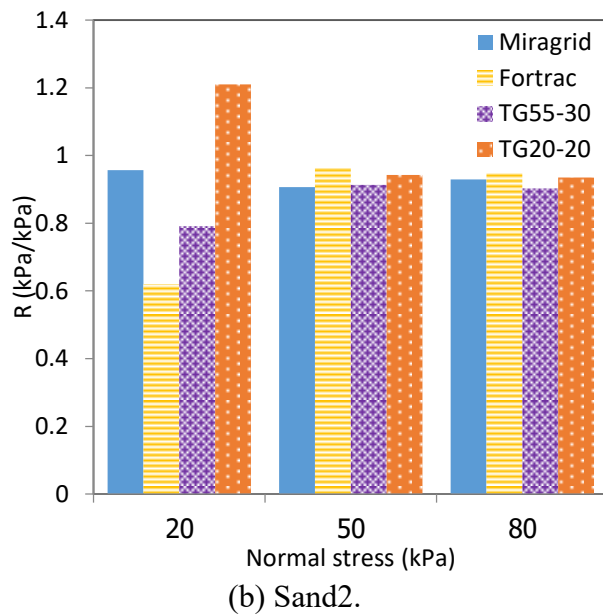


(a) Sand1.

(b) Sand2.

**Fig. 12.** Comparison between the maximum pullout resistance laboratory and numerical analysis.

## 4.2 Pullout resistance in clay

The evaluation of the graphs presented in Fig. 13 reveals that after the dramatically enhancement in the shear force in the first step, a stepping increase is observed. This stepping transpires in the higher displacement as the higher normal stress applying.
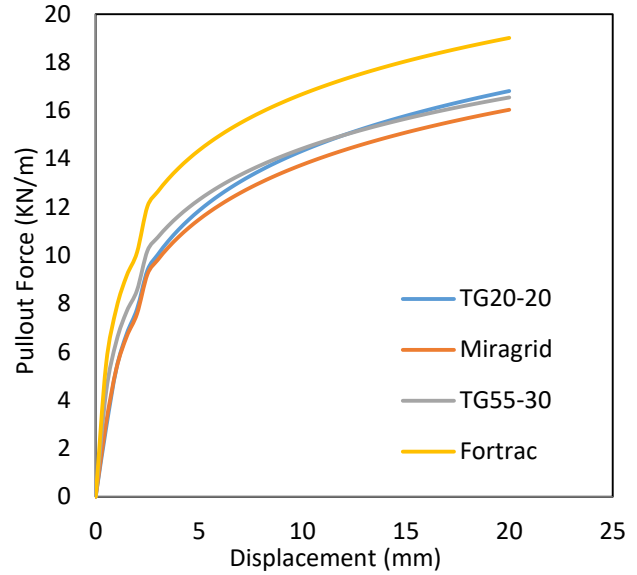


(a) 20 kPa.



(b) 50 kPa.
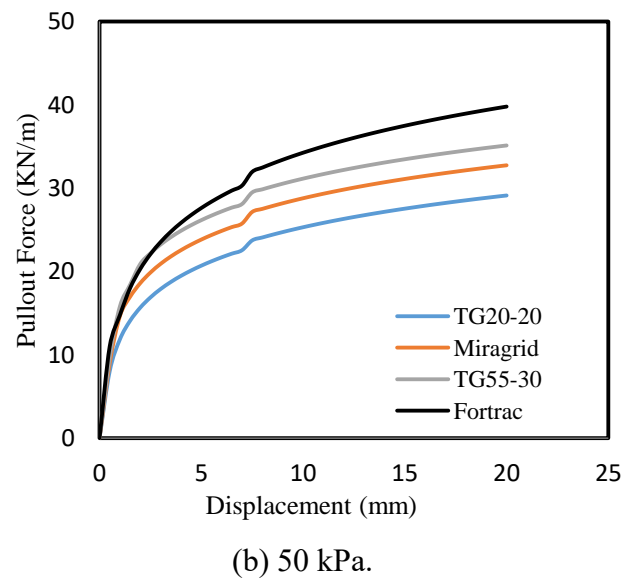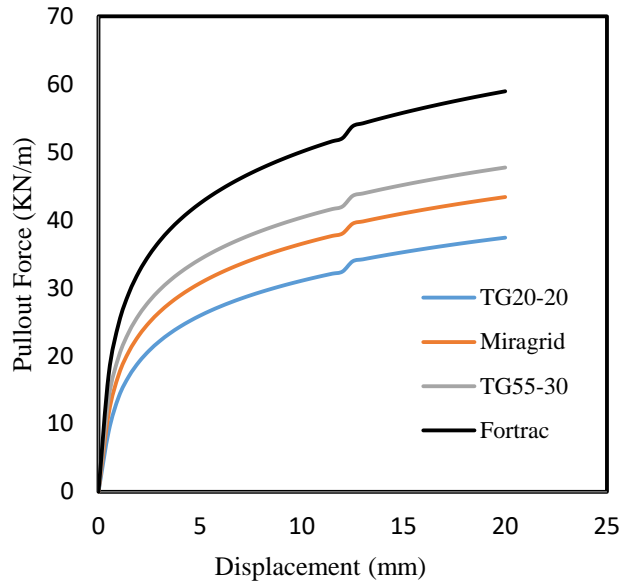
(c) 80 kPa.

**Fig. 13.** Laboratory pullout-displacement results on geogrids with different normal stress applied in clay.

As the huge part of the geogrid interaction resistance is as a result to the passive resistance of the soil in front of the transverse elements, this passive resistance is like the bearing capacity of the foundations. Then again, the punching shear failure of the foundations usually takes place in the dense soils, loose sands and saturated clays. As this clay is dense, one can say that this stepping is because of the punching shear failure. These results also were observed from the pullout tests conducted by Palmeria [21].

The effect of the low normal stress is observable in clays too. In 20 kPa normal stress, the geogrid with the lower strength easily strains. Further, the pullout strength increases in the geogrid with the lower strength due to the friction mobilization. In 50 and 80 kPa stresses, the particles compact and the passive resistance mobilizes.

Numerical results presented in Fig. 14 display that the punching failure only appears in the stiffer geogrid and in the higher displacements than experimental results. It is

also obvious that the pullout force is estimated more conservative than the analysis on sands.
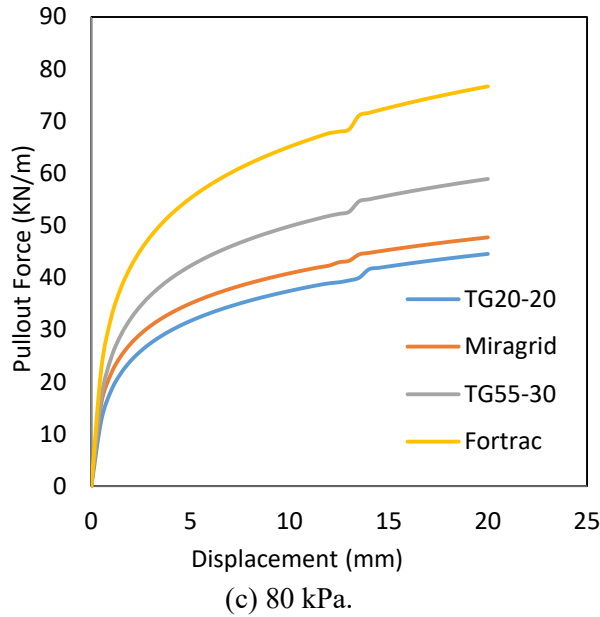


(a) 20 kPa.
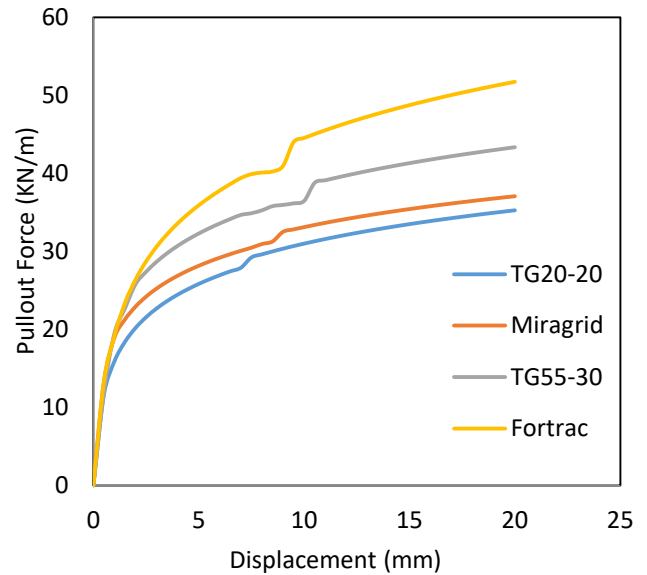


(b) 50 kPa.

(c) 80 kPa.

**Fig. 14.** Numerical pullout-displacement results on geogrids with different normal stress applied in clay.

## 4.3 Effect of particle size of sands on this interaction

The friction angle is one of the major factors that control the geogrid-soil interaction. Sand1 represents the fine sand and the sand2 represents the coarse sand. Fig 15 compares the geogrids in two sands. In Figs. 15a and Fig. 15b, it is clear that sand2 indicates the higher pullout resistance than sand1. Notwithstanding, Figs. 15c and Fig. 15d manifest that the friction angle isn't the only effective parameter and the geogrid thickness also affects the result. Ppursuant to Subaida, Chandrakaran and Sankar, the finer sands have higher pullout resistance and the pullout strength increases if the particles size of sand be close to the geogrid thickness [22].

## 4.4 Effect of type of soil

In Fig. 15, Sand1 has the pullout strength higher than the clay in all conditions. It indicates that all of the geogrids strength doesn't mobilize completely in clays. In
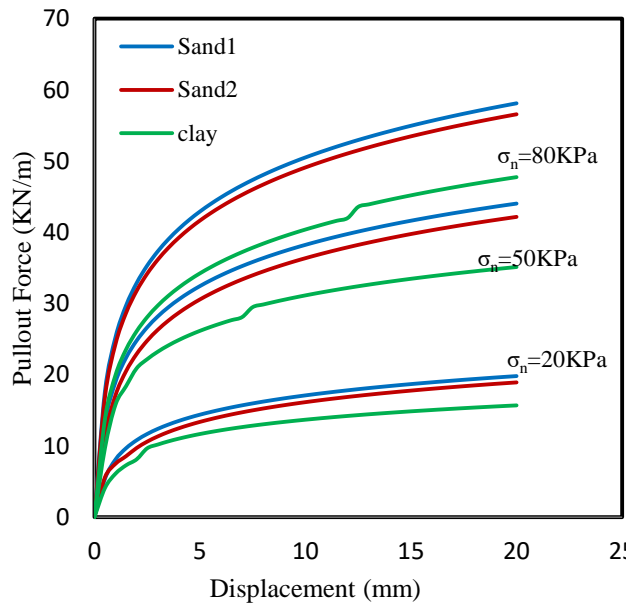
addition, the passive resistance in front of transverse elements increases in sands. Abdi and Arjomand assessed the possibility of using a thin layer of sand around geogrids in clay soils for ameliorating the passive resistance in order to reach the full capacity of the geogrid in clays [6].
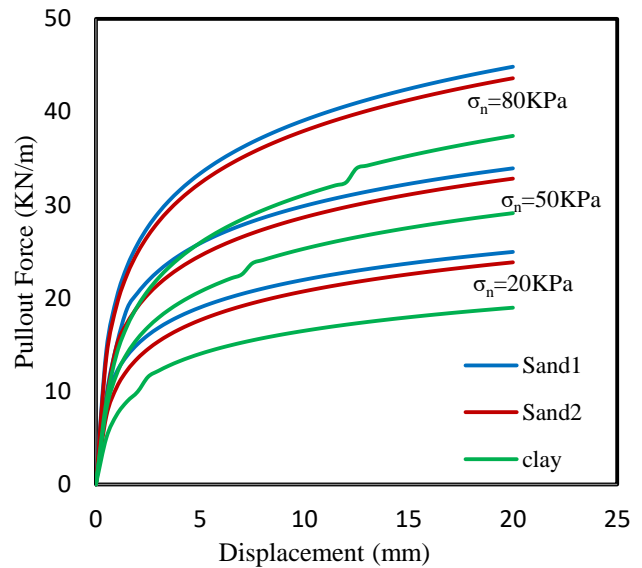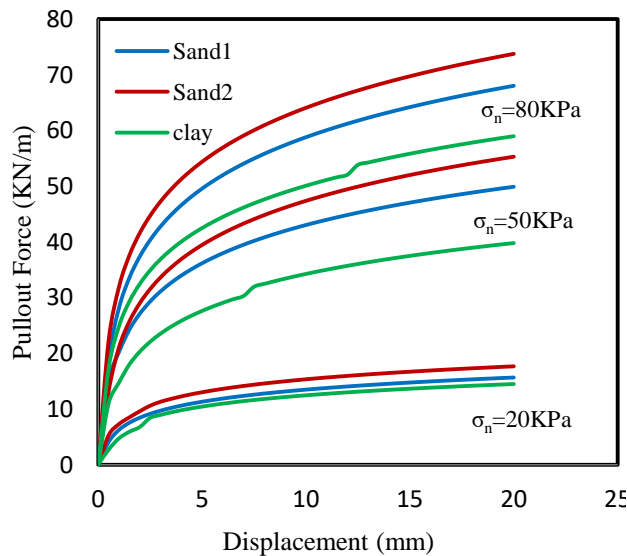


(a) TG20-20.
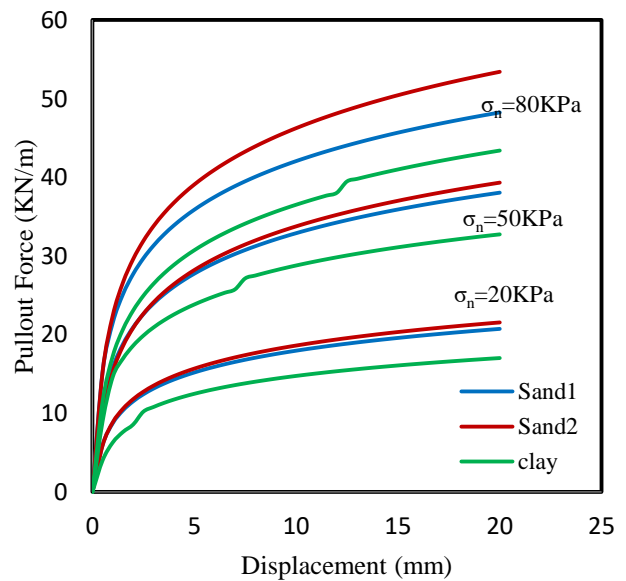


(b) Miragrid.

(c) TG55-30.



(d) Fortrac.

**Fig. 15.** Laboratory pullout resistance in sand, sand2 and clay.

## 5. Conclusion

This study inquired the pullout resistance of the geogrids and the tensile strength effect on this resistance in the granular and cohesive soils with both experimental and numerical approaches. In this investigation, 36 tests were conducted with the reformed direct shear test apparatus in large scale. 4 types of the geogrids were tested and simulated under three normal stresses. Based on this study, the following main conclusions are made:

(1) In 20 kPa normal stress, the geogrid with the lower tensile strength has revealed higher pullout resistance. However, by increasing the normal stress to 50 kPa and 80 kPa, the pullout resistance increase in the geogrid with higher tensile strength in both sands and clays.

(2) The numerical approach doesn't contemplate the geogrid behavior in 20 kPa normal stresses in all soils and the geogrids with higher strength shows higher resistance. Although, in the numerical results have good agreement with experimental analysis under the 50 and 80 kPa normal stresses.

(3) In clays, the punching shear failure took place at the geogrid-soil interface. In the numerical analysis, this failure only indicated in stiffer geogrids. Moreover, the finite difference results in clays were more conservative.

(4) It was found that the enhancement in normal stress has linear relation with the pullout resistance in clay and sands.

(5) The soil particles size, geogrid aperture and thickness of elements are controlling the geogrid-soil interaction behavior. The Increase in the geogrid-soil interaction strength occurs in soil which the size of particles be close to the geogrid thickness

(6) Generally in all tests and simulated models in sands manifested higher pullout strength than clay one.

# REFERENCES

[1] Bergado, D.T., Chai, J.C., Abiera, H.O., Alfaro, M.C., Balasubramaniam. (1993). "Interaction between Cohesive – Frictional Soil and Various Grid Reinforcements". Geotextiles and Geomembranes, Vol. 12, No. 4, pp. 327 – 349.

[2] Korner, R. M. (2005). "Designing with geosynthetic". 5th ed. 338.

[3] Moraci, N., Recalcati, P. (2006). "Factors affecting the pullout behaviour of extruded geogrids embedded in a compacted granular soil". Geotext. Geomembr. 24 (4), 220-242.

[4] Arulrajah, A., Rahman, M.A., Piratheepan, J., Bo, M.W., Imteaz, M.A. (2014). "Evaluation of interface shear strength properties of geogrid-reinforced construction and demolition materials using a modified large-scale direct shear testing apparatus'. J. Mater. Civ. Eng. 26 (5), 974e982.

[5] Lopes, M.L., Ladeira, M. (1996). 'Influence of the confinement, soil density and displacement rate on soil geogrid interaction". Geotext. Geomembr. 14 (10), 543-554.

[6] Abdi, M.R., Arjomand, M.A. (2011). "Pullout tests conducted on clay reinforced with geogrid encapsulated in thin layers of sand". Geotext. Geomembr. 29 (6), 588e595.

[7] Naeini, S.A., Khalaj, M., Izadi, E. (2013). "Interfacial shear strength of silty sandegeogrid composite". Proc. ICE Geotech. Eng. 166 (1), 67-75.

[8] Liu, C.-N., Yang, K.-H., Nguyen, M.D. (2014). "Behavior of geogrid reinforced sand and effect of reinforcement anchorage in large-scale plane strain compression". Geotext. Geomembr. 42 (5), 479-493.

[9] Bergado, D.T., Chai, J.-C. (1994). "Pullout force-displacement relationship of extensible grid reinforcements". Geotext. Geomembr. 13 (5), 295-316.

[10] Ochiai, H., Yasufuku, N., Yamaji, T., Xu, G.-L., Hirai, T. (1996). "Experimental evaluation of reinforcement in geogrid soil structure". In: Proceedings of International Symposium on Earth Reinforcement, Kyushu, Japan, pp. 249-254.

[11] Moraci, N., Cardile, G. (2012). "Deformative behaviour of different geogrids embedded in a granular soil under monotonic and cyclic pullout loads". Geotext. Geomembr. 32, 104-110.

[12] Mosallanezhad, M., Taghavi, S.S., Hataf, N., Alfaro, M. (2016). "Experimental and numerical studies of the performance of the new reinforcement system under pull-out conditions". Geotext. Geomembr. 44 (1), 70-80.

[13] Esfandiari, J., Selamat, M.R. (2012). "Laboratory investigation on the effect of transverse member on pull out capacity of metal strip reinforcement in sand". Geotext. Geomembr. 35, 41-49.

[14] Bathurst, R.J., Ezzein, F.M. (2015). "Geogrid and soil displacement observations during pullout using a transparent granular soil". Geotech. Test. J. 38 (5), 673-685.

[15] Mahmoud, G., Mohamed, A. (2013). "Three dimensional finite element analysis of soil geogrid interaction under pullout loading condition". GeoMonteral, 66th Canadian Geotechnical Conference , 260, 452-458.

[16] Ezzein, F.M., Bathurst, R.J., Kongkitkul, W. (2015). "Nonlinear loadestrain modeling of polypropylene geogrids during constant

rate-of-strain loading". Polym. Eng. Sci. 55 (7), 1617-1627.

[17] Qian, Y., Mishra, D., Tutumluer, E., Kazmee, H.A. (2015). "Characterization of geogrid reinforced ballast behavior at different levels of degradation through triaxial shear strength test and discrete element modeling". Geotex. and Geomembr., 43(5), 393-402.

[18] Wang, Z., Jacobs, F., Ziegler, M. (2016). "Experimental and DEM investigation of geogrid-soil interaction under pullout loads". Geotex. and Geomembr. 44, 230-246.

[19] ASTM D6706-01. (2001). "Standard test method for measuring geosynthetic pullout resistance in soil". Annual Book of ASTM Standards. ASTM International, West Conshohocken, USA.

[20] ASTM D5321, 2017. "Standard Test Method for Determining the Shear Strength of Soil-Geosynthetic and Geosynthetic-Geosynthetic Interfaces by Direct Shear. Annual Book of ASTM Standards". ASTM International, West Conshohocken, USA.

[21] Palmeira, E.M. (2004). "Bearing force mobilisation in pull-out tests on geogrids". Geotext. Geomembr. 22 (6), 481-509.

[22] Subaida, E.A., Chandrakaran, S., Sankar, N. (2008). "Experimental investigations on tensile and pullout behavior of woven coir geotextiles". Geotex. and Geomembr. 26(2008), 384-392.